IJARSCT
ISSN (Online) 2581-9429
International Journal of Advanced Research in Science, Communication and Technology (IJARSCT)
Volume 2, Issue 2, July 2022
Impact Factor: 6.252

Voltage and Frequency Regulation of Isolated System under Unbalanced Condition

Rahul[1] and Sukhbir Singh[2]
M.Tech Scholar, Department of Electrical Engineering[1]
Assistant Professor, Department of Electrical Engineering[2]
School of Engineering & Technology, Soldha, Bahadurgarh, Haryana, India

Abstract: *In this dissertation, a 3-phase 3-wire isolated microgrid system is designed for standalone conditions. The components of the isolated system are wind driven SEIG, solar photovoltaic (SPV), insulated gate bipolar transistor (IGBT) based voltage source converter (VSC), interfacing inductors, energy storage system (ESS) and 3-phase nonlinear load. An EPLL-PLL based control algorithm with VSC is implemented to regulate the voltage, frequency and improve the power quality of the wind-solar hybrid system. Moreover, the proposed control with VSC also provides harmonic compensation, load balancing and reactive power support of the hybrid system. The SPV with battery system is interfaced at DC link of the VSC to provide active and reactive power support under transient conditions. An incremental conductance method is used to extract maximum power from a SPV. The battery system consumes the unused power under varying load demand. The entire system is designed MATLAB/Simulink and results are taken under varying wind speed and varying solar insolation feeding 3-phase nonlinear load.*

Keywords: SEIG**,** voltage source converter, phase locked loop

I. INTRODUCTION

The electronic converter is composed by a three-phase four-wire shunt active filter and a dc chopper attached to its dc bus. The converter compensates the current harmonics, the reactive power and the load unbalances at its ac side and dissipates the active power excess through the chopper at its dc side. The designed control architecture assures that, in steady state, the RMS values of the voltages and the frequency remain at the their reference values [1]. A new strategy for controlling voltage and frequency of a self excited induction generator (SEIG) is presented [2]. The STATCOM is employed to compensate the unbalanced currents caused by single-phase loads that are connected across the two terminals of the three-phase SEIG. Therefore, the SEIG is capable of feeding single-phase loads up to its rated power. Moreover, the STATCOM regulates the SEIG terminal voltage through reactive power compensation and also suppresses the harmonics injected by consumer loads [3]. The problem of voltage dip arising from varying loads is reduced with use of STATCOM along with fixed excitation. The shunt excitation capacitor needs to supply the reactive power of demand of SEIG to generate rated voltage at no-load [4]. The employed SSSC is a three-phase, Insulated Gate Bipolar Transistor (IGBT) based, PWM operated, Current-Control Voltage source converter (CC-VSC). The reference current to generate the gating signals is obtained by employing only one PI control loop [5]. A three-phase insulated gate bipolar junction transistor (IGBT) based current controlled voltage source converter (CCVSC) with a dc bus capacitor is used to regulate the magnitude of the generated voltage along-with its functioning as a harmonic eliminator and a load balancer [6, 7]. An approach based on three-phase induction machine model is employed to derive dynamic equations of the studied SEIG. Steady state characteristics such as unbalanced voltage factor, unbalanced current factor and efficiency of studied SEIG are examined and compared for three different passive loads and three kinds of neutral connection [8]. A general analysis to predict the steady state performance of an isolated self excited induction feeding a balanced R-L load is presented [9]. The CC-VSC with PV system fulfills the requirement of reactive and active power of integrated system [10]. DC offset in the input of phase-locked loops (PLLs) is a challenging problem since it will result in fundamental frequency oscillations in the estimated phase and frequency [11]. An automatic voltage regulator (AVR) is used to regulate the output voltage of the DG to the desired value [12]. A Perturb and Observe (P&O) method is used to achieve the Maximum Power Point Tracking (MPPT) from the WT without using speed sensors. Two levels of control are proposed for the threephase voltage source inverter for voltage and frequency regulation at the Point of

IJARSCT
ISSN (Online) 2581-9429
International Journal of Advanced Research in Science, Communication and Technology (IJARSCT)
Volume 2, Issue 2, July 2022
Impact Factor: 6.252

Common Coupling (PCC) and power management in standalone and diesel connected modes [13]. An MSOGI-based control algorithm is used for load balancing, harmonics elimination, and power factor correction and delivering active power to the grid. The MSOGI-FLL has advantages of adaptive nature with frequency variation and better harmonics filtering capabilities when compared with conventional algorithms, which is demonstrated with frequency domain analysis [14]. The INC control is used to harvest the PV array maximum power. For controlling the voltage output of the DEGS, an electronic automatic voltage regulator (AVR) is provided at the synchronous generator (SG) field winding. The neutral current compensation is achieved by controlling the fourth-leg of VSC [15]. A CC-ROGI-FLL also extricates the fundamental grid voltages component even under grid voltage harmonic distortion and grid voltages unbalancing [16].

II. System Description

The components of the isolated microgrid system in which wind turbine used as a prime mover of SEIG, VF controller integrated with PV array, VF controller (consisting of 3 legs CC-VSC, PV array at DC link and energy storage system) and linear/nonlinear load at the consumer end. A star type capacitor bank of 3-phase is used for induction generators self-excitation purpose and for producing the no load rated voltage have to choose the excitation capacitor value. The energy storage system (ESS) at DC link is used for the consumption of surplus power. PV system maintains constant active power of SEIG when variation in wind speed and load demand increases. The generated voltage and frequency of SEIG will remain in limit during the change in load demand. The AC filter inductors are connected between the SEIG terminals and the output of the STATCOM. The VSC connected with DC linked capacitor for providing self supporting type DC bus filter voltage ripples. According to the changes in load demand, the surplus power is consumed by ESS.

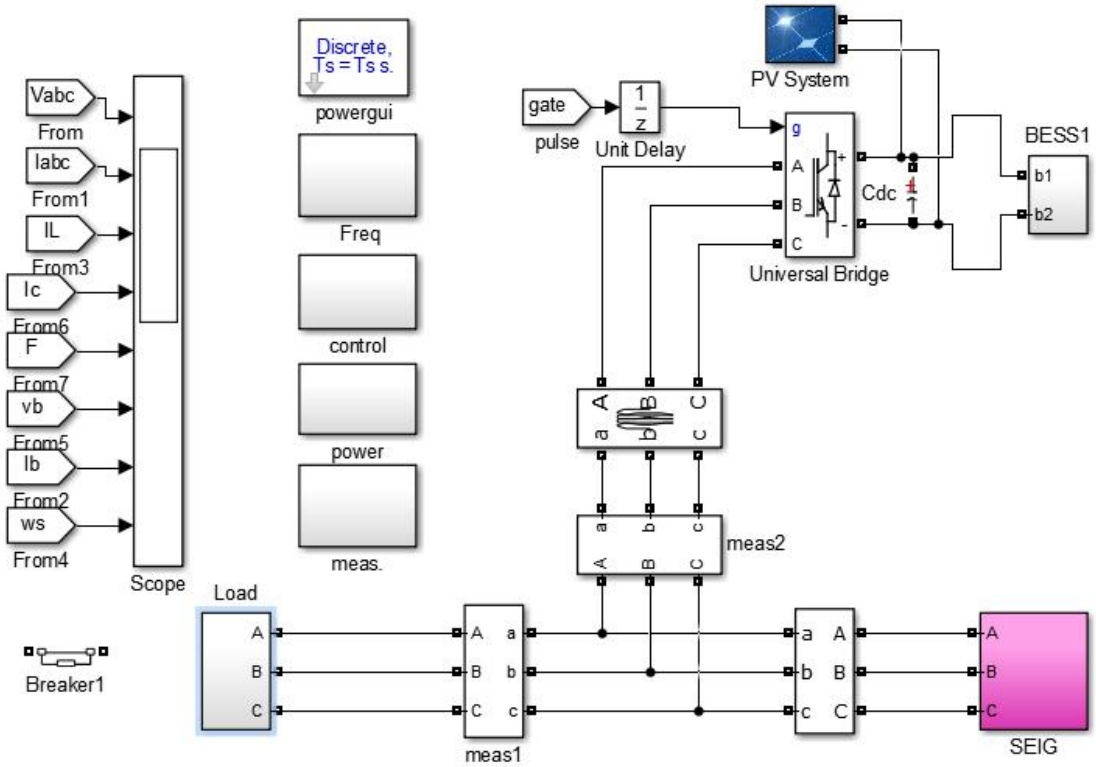

Figure 1 Schematic of isolated microgrid system

III. Research Methodology

The schemes control process is depend on reference source current generation has two components of AC voltage with in-phase and at quadrature axis. Controller in-phase unity templates have three phase sinusoidal functions are (ua, ub and uc). The AC terminal voltage (V_t) of wind driven SEIG is sensed and compared with the reference voltage (V_{tref}).

IJARSCT
ISSN (Online) 2581-9429
International Journal of Advanced Research in Science, Communication and Technology (IJARSCT)
Volume 2, Issue 2, July 2022
Impact Factor: 6.252

The voltage error is processed in the AC voltage PI controller. The output of the PI controller for AC voltage control loop decides the amplitude of reactive current (I^*_{smq}) which yields the quadrature component of the reference source currents (i^*_{saq}, i^*_{sbq} and i^*_{scq}). For constant power application, active power component of source currents are fixed at rated value, which is the amplitude of in phase component of source current (I^*_{smd}). Multiplication of in-phase unit templates (u_a, u_b and u_c) with in phase component of the reference source currents (I^*_{smd}) yields the in-phase component of the reference source currents (i^*_{sad}, i^*_{sbd} and i^*_{scd}). The sum of instantaneous quadrature and in-phase components of current is the reference source currents (i^*_{sa}, i^*_{sb} and i^*_{sc}), which are compared with the sensed source currents (i_{sa}, i_{sb} and i_{sc}). These current error signals are amplified and compared using PWM hysteresis controller for generating the PWM signal for switching of the devices of CC-VSC. Fourth leg of voltage source converter (VSC) is used to compensate the source neutral current (i_{sn}) and its reference value is taken zero (i^*_{sn}) through switching neutral connection. The excess generated power other than consumer load is consumed in ESS [7-9].

CC-VSC Control Scheme

The control scheme modeling for the 4-leg CC-VSC and wind turbine for VF control along with PV system is estimated as follows:

Evaluation of in phase component of reference source current:

Wind driven SEIG integrated with PV system will generate constant active power to feed either consumer load or BESS for the constant active power generation, which is estimated as:

$$\boldsymbol{I^*_{smd} = \sqrt{2}\, P_{rated}/\sqrt{3}\, V_{rated}} \quad (1)$$

Where P_{rated} is the rated power and V_{rated} is the rated voltage of SEIG and I^*_{smd} is peak value of rated active current of SEIG. At SEIG terminal the instantaneous line voltages (v_a, v_b and v_c) are assumed sinusoidal and corresponding maximum value is calculated as:

$$V_t^2 = \{(2/3)(v_a^2 + v_b^2 + v_c^2)\} \quad (2)$$

The unity in phase is derived from templates having instantaneous voltage as follows:

$$u_a = v_a/V_t\ ;\ u_b = v_b/V_t\ ;\ u_c = v_c/V_t \quad (3)$$

In-phase components in the form of Instantaneous values of reference source currents are calculated as:

$$i^*_{sad} = I^*_{smd}u_a\ i^*_{sbd} = I^*_{smd}u_b\ i^*_{scd} = I^*_{smd}u_c \quad (4)$$

Evaluation of quadrature component of reference source current:

The voltage error (v_{er}) at SEIG terminal at the n^{th} sampling instant calculated as:

$$\boldsymbol{v_{er(n)} = v_{tref(n)} - v_{t(n)}} \quad (5)$$

Where $v_{tref(n)}$ is the reference peak voltage and $v_{t(n)}$ is the peak value of the sensed 3-phase voltage at the SEIG terminals at the n^{th} sampling instant is calculated as:

$$i^*_{smq(n)} = i^*_{smq(n-1)} + k_{pa}\{v_{er(n)} - v_{er(n-1)}\} + k_{ia(n)}v_{er(n)} \quad (6)$$

Where k_{pa} is the proportional gain and k_{ia} is the integral gain constants of the PI voltage controller. $v_{er(n)}$ is the voltage errors for n^{th} instant and $v_{er(n-1)}$ is the voltage errors for $(n-1)^{th}$ instant and $I^*_{smq(n-1)}$ is the maximum value of quadrature component of the reference source current at $(n-1)^{th}$ instant. The quadrature components of the reference source currents for instantaneous values are calculated as:

$$i^*_{saq} = I^*_{smq}w_a,\ i^*_{sbq} = I^*_{smq}w_b,\ i^*_{scq} = I^*_{smq}w_c \quad (7)$$

Where (w_a, w_b and w_c) are the unit vectors having a 90^0 of phase change with respect to unit templates (u_a, u_b and u_c) are given below:

$$w_a = -u_b/\sqrt{3} + u_c/\sqrt{3} \quad (8)$$

$$w_b = \sqrt{3}\,u_a/2 + (u_b - u_c)/2\sqrt{3} \quad (9)$$

$$w_c = -\sqrt{3}\,u_a/2 + (u_b - u_c)/2\sqrt{3} \quad (10)$$

IJARSCT
ISSN (Online) 2581-9429
International Journal of Advanced Research in Science, Communication and Technology (IJARSCT)
Volume 2, Issue 2, July 2022
Impact Factor: 6.252

Evaluation of total reference source current:

The total reference source currents are sum of the reference source current's in-phase and quadrature components calculated as:

$$i^*_{sa} = i^*_{saq} + i^*_{sad} \quad (11)$$

$$i^*_{sb} = i^*_{sbq} + i^*_{sbd} \quad (12)$$

$$i^*_{sc} = i^*_{scq} + i^*_{scd} \quad (13)$$

PWM current controller for 3-leg VSC:

Comparison of the reference source currents ($\boldsymbol{i^*_{sa}, i^*_{sb}}$ ***and*** $\boldsymbol{i^*_{sc}}$) with the sensed source currents ($\boldsymbol{i_{sa}, i_{sb}}$ ***and*** $\boldsymbol{i_{sc}}$). The PWM current controllers generate the ON / OFF switching patterns for the gate drive signals to the IGBTs. The current error is calculated as:

$$i^*_{saerr} = i^*_{sa} - i_{sa} \quad (17)$$

$$i^*_{sberr} = i^*_{sb} - i_{sb} \quad (18)$$

$$i^*_{scerr} = i^*_{sc} - i_{sc} \quad (19)$$

The amplified current error signals are compared with triangular carrier wave. If the amplified current error signal corresponding to phase A (i_{saerr}) is greater than the triangular wave signal switch S4 is ON and the switch S1 is OFF and the switch feature SA is set to 0. If the corresponding amplified current error signal (i_{saerr}) is equal to or less than the triangular wave signal switch S1 and switch S4 is OFF, and the value of SA is set to similar logic applied to other phases.

Design of Wind Turbine

The selection of proper wind turbine rating is extremely important which is working as a prime mover for an isolated asynchronous generator (IAG). The available mechanical power for energy conversion is dependent on power coefficient (c_p), wind velocity (v_w), area of the blade (a). The power output equation written as:

$$P = \frac{1}{2} c_p(\eta, \beta) \pi r^2 v_w^3 \quad (20)$$

Where r, v_w, β are the radius of blade (m), wind speed (m/s), the air density (kg/m^3) respectively. The performance coefficient varies with the wind speed, angular speed of generator, angle of attack and pitch angle. c_p is dependent on tip speed ratio and blade pitch angle, θ (deg). The tip speed ratio (η) is given as:

$$\eta = \frac{\omega_R r}{v_w} \quad (21)$$

Where, $\omega_R$is the angular velocity in rad/s.

Control of the energy storage system (EES) system

The battery is designed for the consumption of surplus power other than consumer load. The figure 6 shows the simulink diagram of battery energy system. The battery is designed by using capacitor, the capacitance can be calculated as:

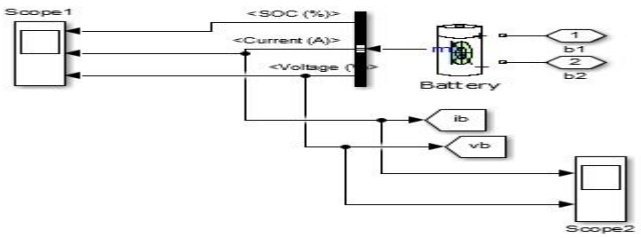

Figure 2 Simulink diagram of battery energy system (BES)

$$C_B = \frac{kWh \times 3600 \times 10^3}{0.5(V^2_{ocmax} - V^2_{ocmin})} \quad (22)$$

The battery model shown in fig. 2, R_s is the equivalent resistance of parallel/series combination of a battery, which is usually a small value. R_B and C_B is used to describe the stored energy in parallel circuit and voltage during charging and discharging. V_{ocmax} and V_{ocmin} are represents the voltage variation across the battery.

IJARSCT
ISSN (Online) 2581-9429
International Journal of Advanced Research in Science, Communication and Technology (IJARSCT)
Volume 2, Issue 2, July 2022
Impact Factor: 6.252

Control of PV system

The PV system is connected at DC link for the implementation of maximum power point tracking (MPPT). The PV array block has two inputs that are used to varying sun irradiance (input 1 in W/m^2) and temperature (input 2 in deg. C). The switching duty cycle is optimized by an MPPT controller which uses the technique of incremental conductance and integral regulation. The integral regulator minimizes the error. To generate required voltage, MPPT system is used to vary the duty cycle automatically. The MPP can be expressed by using the relation between dI/dV and –I/V. The voltage depends on the photovoltaic current, then on the power P = I(V)×I. The figure 7 represents the simulink diagram of PV system.

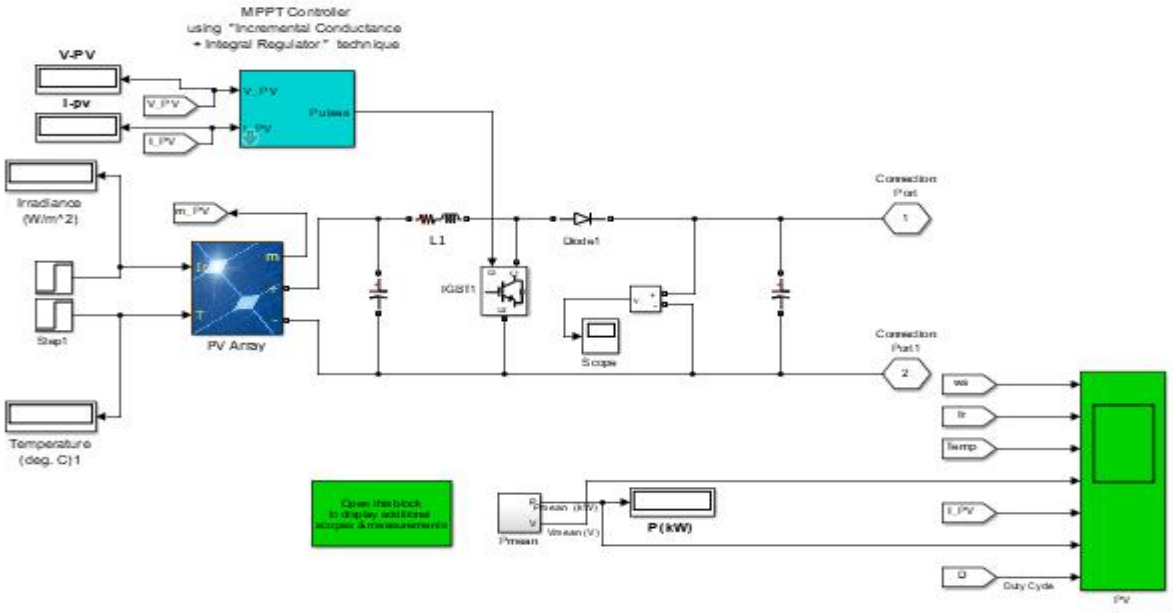

Figure 3 Simulink diagram of PV system

Hence,

$$dP/dV=V\times(dI/dV)+ I(V). \quad (23)$$

Where, dP/dV represents the incremental conductance and -I/V represents instantaneous conductance. When, dP/dV=0, then, dI/dV=-I(V)/V. Thus, the IC is equivalent to the negative of the instantaneous conductance. The dI/dV= -I(V)/V voltage is known as MPP voltage. This voltage is controlled by the controller until the solar irradiation adjusts and the process repeats. The error signal (e) is estimated as:

$$e= I/V+ dI/dV \quad (24)$$

The residual steady state error is reduced by an integral controller. A proportional integral used to decrease signal error.

IV. RESULTS AND DISCUSSION

The simulation result shows the performance of isolated microgrid system under varying wind speed/solar irradiation feeding 3-phase nonlinear load. An EPLL-PLL based control with VSC maintains the source voltage, source current, load current, compensator current, and system frequency under different operating conditions.

4.1 Dynamic Performance of Isolated System under Varying Wind Speed

The simulation result shows the performance of isolated microgrid system under different operating conditions. Figure 4(a) shows the source voltage, source current, load current and controller current are effectively maintain by proposed control. The proposed control with VSC regulates the system frequency, voltage and enhances the power quality of the wind solar hybrid system. The control also provides harmonic compensation, active and reactive power support and load leveling to the hybrid system.

IJARSCT
ISSN (Online) 2581-9429
International Journal of Advanced Research in Science, Communication and Technology (IJARSCT)
Volume 2, Issue 2, July 2022
Impact Factor: 6.252

Figure 4(b) shows the variation in wind speed 19 m/s to 14 m/s. The controller maintains the voltage stable under varying wind speed. During this duration the controller provides active power support at common point of interfacing (CPI). The battery charging current is reduced due to reduction in wind speed.

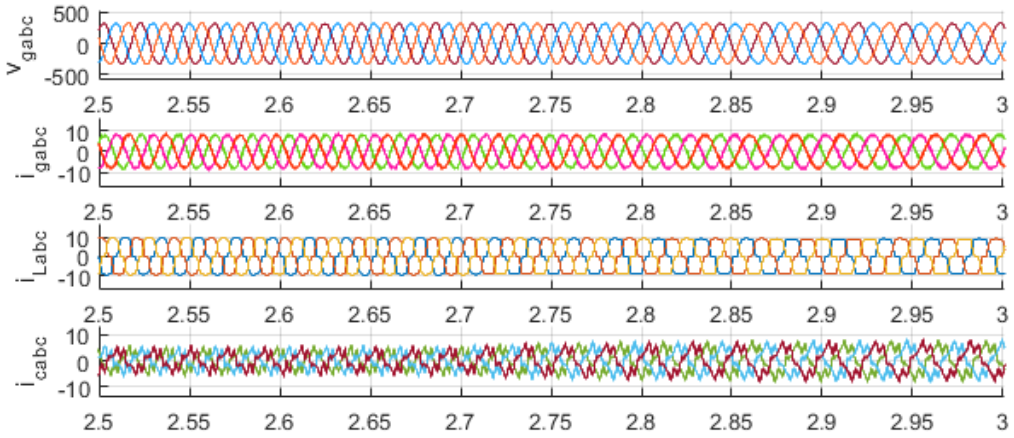

(a)

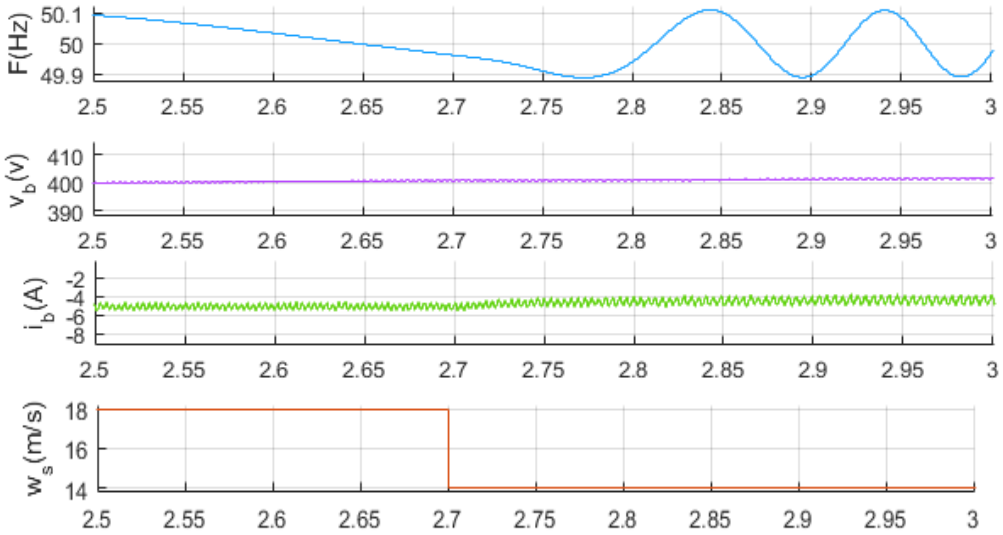

(b)

Figure 4(a) and (b) Dynamic performance of isolated microgrid system at varying wind speed

4.2 Dynamic Performance of Isolated Microgrid System under varying Solar Insolation

Figure 5(a) and (b) shows the simulation results of isolated microgrid system under fixed wind speed and varying solar insolation feeding three phase nonlinear load. Figure 5(a) shows the source voltage, source current, load current and controller current under fixed wind speed and varying solar irradiation feeding 3-phase nonlinear load. The simulation result shows the affectivity of the controller. The controller maintains the frequency, voltage and stability of the isolated system under different operating conditions.

Figure 5(b) shows the system frequency, battery voltage, battery current, solar irradiation and temperature. The solar insolation and temperature are varying from 900 w/m^2 to 700 w/m^2 and 25°C to 20°C. During variation in solar insolation, the extra power is supplied by the battery energy system to provide power support at CPI.

IJARSCT
ISSN (Online) 2581-9429
International Journal of Advanced Research in Science, Communication and Technology (IJARSCT)
Volume 2, Issue 2, July 2022
Impact Factor: 6.252

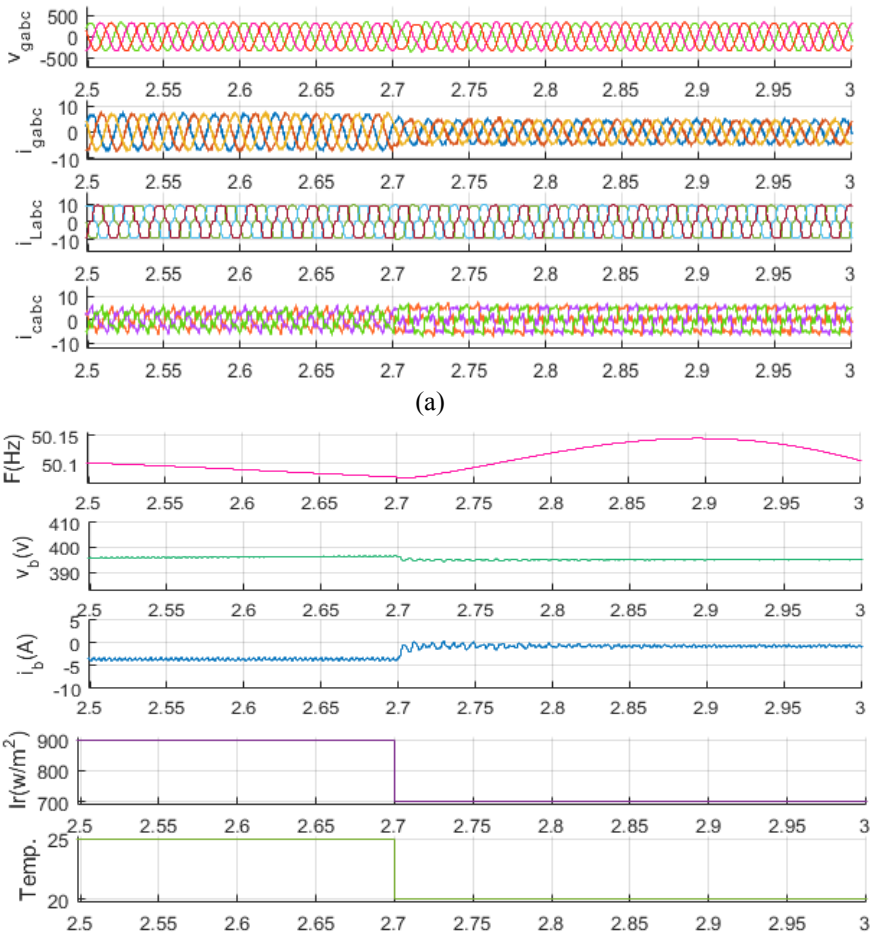

(a)

(b)

Figure 5(a) and (b) Dynamic response of isolated microgrid system at varying solar insolation

4.3 Dynamic response of Isolated Microgrid System under unbalanced load

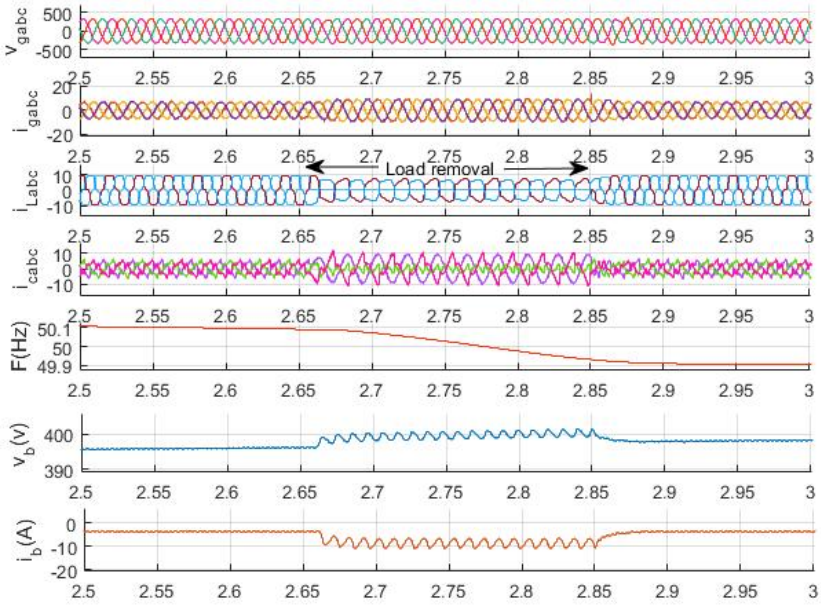

Fig. 6 Dynamic response of isolated microgrid system under unbalanced load

IJARSCT
ISSN (Online) 2581-9429
International Journal of Advanced Research in Science, Communication and Technology (IJARSCT)
Volume 2, Issue 2, July 2022
Impact Factor: 6.252

Fig. 6 shows the dynamic performance of standalone hybrid system under fixed wind speed/solar intensity feeding varying linear/nonlinear load. The phase 'a' of linear/nonlinear load is disconnected at t=2.65 sec to t=2.85 sec., then the PCC current is sinusoidal and balanced. During this duration, the CPI current, compensator current, and battery current is increasing and load current is decreasing. The controller maintains the CPI voltage and frequency are constant. As under removal of load one phase 'a', there is a reduction in load requirement, and the excess power, which is earlier supplying to the load, is fed to the battery. Thus, there is an escalation in the battery current (+ ve direction).

V. Conclusion and Future Scope

A 3-phase 3-wire wind-solar hybrid system is designed to generate power for standalone conditions. The components of the hybrid system are wind driven SEIG, solar photovoltaic (SPV), insulated gate bipolar transistor (IGBT) based voltage source converter (VSC), interfacing inductors, energy storage system (ESS) and 3-phase nonlinear load. The interfacing inductors are used to reducing the ripples. An EPLL-PLL based control algorithm with VSC is effectively regulates the voltage, frequency and improves the power quality of the wind-solar hybrid system. The proposed control with VSC also provides harmonic compensation, load balancing and reactive power support of the hybrid system. The SPV with battery system is interfaced at DC link of the VSC to provide active and reactive power support under dynamic conditions. The battery system consumes the extra power under varying load demand or less load demand. The entire system is designed MATLAB/Simulink under different operating conditions.

Over the last few years, microgrid deployments throughout the world have increased. Connected products allow a microgrid owner to feed energy to the main grid or island. Digital controls can also optimize energy production. Overall, microgrids are helping society achieve a decarbonized, decentralized, digitized energy future.

REFERENCES

[1]. J. A. Barrado and Robert Grino, "Voltage and frequency control for a self excited induction generator using a three ohase four wire electronic converter" 1-4244-0121-6, IEEE 2006

[2]. E. Suarez and G. Bortolotto, "Voltage-frequency control of a self excited induction generator" IEEE transaction on energy conversion, vol. 14, no. 3, sept. 1999

[3]. Bhim Singh, S. S. Murthy and R. S. Reddy Chillipi, "STATCOM based controller for a three phase SEIG feeding single phase loads" IEEE transaction on energy conversion, vol. 29, no. 2, june 2014

[4]. Bhim Singh, Madhusudan, Vishal Verma and A. K. Tandon, "Rating reduction of static compensator for voltage control of three phase self excited induction generator" IEEE ISIE, July 2006

[5]. Y. K. Chauhan, S. k. Jain and Bhim singh, "Performane of a three phase self excited induction generator with static synchronous series compensator" 978-1-4244-7781-4, IEEE 2010

[6]. Gaurav kumar Kasal and Bhim Singh, "Harmonic elimination, voltage control and load balancing in an isolated power generation" European Transactions on electrical power, june 2009

[7]. L. Shridhar, Bhim Singh, C.S. Jha and B.P. Singh, "Analysis of self excited induction generator feeding inuction motor" IEEE transaction on energy conversion, vol. 9, no. 2, june 1994

[8]. L. Wang and Sung-Chun Kuo, "Steady state performance of a self excited induction generator under unbalanced load" 0-7803-7322-7, IEEE 2002

[9]. N. H. Malik and S. E. haque, "Steady state analysis and performance of an isolated self excited induction generator" IEEE transaction on energy conversion, vol. EC-1, no. 3, Sept. 1986

[10]. S. Sombir and Madhusudan Singh, "Voltage and frequency control of self excited induction generator integrated with PV system" IEEE 2020, 978-1-7281-5414-5/20

[11]. Menxi Xie, Huiqing Wen, Canyan Zhu and Yong Yang, "DC offset rejection improvement in single-phase SOGI-PLL algorithms: Methods review and experimental evaluation" IEEE access, June 2017

[12]. V. Narayanan, Seema Kewat, and Bhim Singh, "Standalone PV-BES-DG based microgrid with power quality improvement" 2019 IEEE International Conference on Environment and Electrical Engineering and 2019 IEEE Industrial and Commercial Power Systems Europe, August 2019, italy, DOI: 10.1109/EEEIC.2019.8783251

[13]. F. Dubuisson, M. Rezkallah, Ambrish Chandra, Marouf Saad, Marco Tremblay and H. Ibrahim, "Control of

IJARSCT
ISSN (Online) 2581-9429
International Journal of Advanced Research in Science, Communication and Technology (IJARSCT)
Volume 2, Issue 2, July 2022
Impact Factor: 6.252

hybrid wind-diesal standalone micro-grid for water treatment system application" Transactions on industry applications, 0093-9994, IEEE 2019

[14]. Priyank Shah, Ikhlaq Hussain and Bhim Singh, "Multi-resonant FLL-based cotrol algorithm for grid interfaced multifunctional solar energy conversion system" IET science, measurement & technology, Volume 12, Iss1ue , January 2018, p. 49 – 62, DOI: 10.1049/iet-smt.2017.0096

[15]. V. Narayanan, Seema Kewat and Bhim Singh, "Control and implementation of a multifunctional solar PV-BES-DEGS based microgrid" IEEE Transactions on Industrial Electronics, august 2020, DOI: 10.1109/TIE.2020.3013740

[16]. Abhishek Kumar, Seema Kewat, Bhim Singh, and Rashmi Jain, "CC-ROGI-FLL based control for grid tied photovoltaic system at abnormal grid conditions" IET generation, transmission & distribution, Volume 14, Issue 17, 04 September 2020, p. 3400 – 3411, DOI: 10.1049/iet-gtd.2019.0765